Mon. Not. R. Astron. Soc. **314**, 87–91 (2000)

The discovery of the optical/IR counterpart of the 12-s transient X-ray pulsar GS 0834−43

G. L. Israel,[1★†] S. Covino,[2] S. Campana,[2†] V. F. Polcaro,[3] P. Roche,[4] L. Stella,[1†] A. Di Paola,[1] D. Lazzati,[2,5] S. Mereghetti,[6] E. Giallongo,[1] A. Fontana[1] and F. Verrecchia[7]
[1]*Osservatorio Astronomico di Roma, Via Frascati 33, I-00040 Monteporzio Catone (Roma), Italy*
[2]*Osservatorio Astronomico di Brera, Via E. Bianchi 46, I-23807 Merate (Lecco), Italy*
[3]*Istituto di Astrofisica Spaziale, Area di Ricerca di Roma–Tor Vergata, Via Fosso del Cavaliere, I-00133 Roma, Italy*
[4]*Deptartment of Physics & Astronomy, University of Leicester, Leicester*
[5]*Dipartimento di Fisica, Università degli Studi, via Celoria 13, I-20133 Milano, Italy*
[6]*Istituto di Fisica Cosmica 'G. P. S. Occhialini' del CNR, Via Bassini 15, I-20133 Milano, Italy*
[7]*Università 'La Sapienza', Dipartimento di Fisica 'Guglielmo Marconi', Piazzale A. Moro 5, I-00185 Roma, Italy*

Accepted 1999 December 3. Received 1999 November 30; in original form 1999 September 9

ABSTRACT

We report the discovery of the optical counterpart of the 12.3-s transient X-ray pulsar GS 0834−43. We reanalysed archival *ROSAT* PSPC observations of GS 0834−43, obtaining two new refined positions, ~14 and ~18 arcsec away from the previously published one, and a new spin period measurement. Based on these results we carried out optical and infrared (IR) follow-up observations. Within the new error circles, we found a relatively faint ($V = 20.1$) early-type reddened star ($V - R = 2.24$). The optical spectrum shows a strong Hα emission line. The IR observations of the field confirm the presence of an IR excess for the Hα-emitting star ($K' = 11.4$, $J - K' = 1.94$), which is likely surrounded by a conspicuous circumstellar envelope. Spectroscopic and photometric data indicate a B0–2 V–IIIe spectral type star located at a distance of 3–5 kpc and confirm the Be-star/X-ray binary nature of GS 0834−43.

Key words: binaries: general – stars: emission-line, Be – pulsars: individual: GS 0834−43 – infrared: stars – X-rays: stars.

1 INTRODUCTION

Be/X-ray binary systems (BeXBs) represent the majority of the known high-mass X-ray binaries (HMXBs) hosting an accreting rotating magnetic neutron star (White, Nagase & Parmar 1995). Phenomenologically, in the X-ray band, BeXBs can be divided into at least three subclasses: (i) bright transients that display giant X-ray outbursts up to $L_X = 10^{38}$ erg s^{-1} (Type II; Stella, White & Rosner 1986) unrelated with the orbital phase, with high spin-up rates, (ii) transients that display periodic outbursts of relatively high luminosity ($L_X \simeq 10^{36}$–10^{37} erg s^{-1}; Type I), generally occurring close to the periastron passage of the neutron star, and (iii) sources displaying no outbursts, but comparatively moderate variations (up to a factor of ~10–100) and low-luminosity ($\leqslant 10^{36}$ erg s^{-1}) pulsed persistent emission (Negueruela 1998). 4U 0115+634 ($P = 3.6$ s), V 0332+30 ($P = 4.4$ s) and EXO 2030+375 ($P = 41.7$ s) are all examples of the first two classes. Among the latter group, there are the well-known X-ray pulsators X Per ($P = 835$ s) and RX J0146.9+6121 ($P = 1455$ s). Moreover, differences between the Galaxy and the Magellanic Cloud populations of BeXBs have been studied and are probably caused by the different star formation rate (see Stevens, Coe & Buckley 1999). B-emission (Be) spectral type stars are characterized by high rotational velocities (up to 70 per cent of their break-up velocity), and by episodes of equatorial mass ejection which might produce a rotating ring of gas around the star at irregular time intervals. At optical wavelengths, Be stars are difficult to classify because of the presence of the circumstellar envelope responsible for the emission lines.

The hard X-ray transient GS 0834−43 ($l_{II} \sim 262.0$, $b_{II} \sim -1.51$) was discovered by the Wide Angle Telescope for Cosmic Hard X-rays (WATCH) experiment on board *GRANAT* in 1990 at a flux level of about 1 Crab in the 5–15 keV energy band (Sunyaev 1990). The source was later observed by *Ginga* (Makino 1990a, 1990b) and *ROSAT* as a part of the All-Sky Survey (Hasinger, Pietsch & Belloni 1990), providing a much better positional accuracy (radius of 50 arcsec). Moreover pulsations at a period of 12.3 s were observed during the *Ginga*, *ROSAT* and ART–P/*GRANAT* observations (Makino 1990c; Aoki et al. 1992; Hasinger et al. 1990; Grebenev & Sunyaev 1990). A *ROSAT* pointing performed in 1991 May allowed the source position to be

★ E-mail: gianluca@coma.mporzio.astro.it
† Affiliated to ICRA.

determined with an uncertainty radius of 9 arcsec (Belloni et al. 1993). An optical follow-up observation of the stars within this error circle was performed at the ESO New Technology Telescope (NTT) in 1991 January: no plausible optical counterpart was found down to a limiting magnitude of $R \sim 23.5$ (Belloni et al. 1993).

GS 0834−43 was also monitored by the Burst And Transient Source Experiment (BATSE) on the Compton Gamma Ray Observatory (*CGRO*) between 1991 April and 1998 July. In particular, seven outbursts were observed from 1991 April and 1993 June with peak and intra-outburst flux of about 300 mCrab and <10 mCrab, respectively (Wilson et al. 1997). The recurrence time of 105–115 d was interpreted as the orbital period of the system. However, no further outbursts have been observed since 1993 July, either with *CGRO*/BATSE or the All Sky Monitor (ASM) on board the *Rossi X-ray Timing Explorer* (*RXTE*). All these findings suggested that GS 0834−43 is a new Be-star/X-ray binary system in an eccentric orbit (Wilson et al. 1997). However, the lack of any plausible optical counterpart remained a key argument against this interpretation.

In this paper we report the discovery of the optical counterpart of GS 0834−43, a $V = 20.4$ Be spectral type star. Starting from three public *ROSAT* PSPC observations of GS 0834−43, we obtained two new independent position measurements (uncertainty radius of 10 arcsec). Within these new error circles we found a highly reddened star ($V - R = 2.24$), the optical spectrum of which shows a strong Hα emission line. The optical counterpart was also observed in the IR, showing that this star is by far the brightest object in the field ($K' = 11.4$). Our findings, obtained from observations in three different energy bands, together support the Be-star/X-ray binary nature of GS 0834−43.

2 X-RAY OBSERVATIONS

The PSPC (0.1–2.4 keV) detector on board *ROSAT* observed the field including GS 0834−43 several times. In the *ROSAT* public archive there are five observations performed between 1991 April and December. PSPC images were accumulated in the 0.5–2.0 keV range in order to reduce the strong and spatially inhomogeneous local background, dominated by the soft X-ray emission from the Vela supernova remnant.

Both a sliding cell and a wavelet transform-based detection algorithm were used in order to characterize the physical parameters [position, count rate, signal-to-noise (S/N) ratio, etc.] of GS 0834−43 when detected, and to obtain a 3σ count rate upper limit in case of non-detection (Campana et al. 1999; Lazzati et al. 1999). Table 1 summarizes the results of this analysis.

GS 0834−43 was detected in 1991 May and December observations as a highly variable source: from 0.067 count s^{-1} (May 5) up to 1.14 count s^{-1} (December 21), corresponding to a variation of a factor of ~20. We note that the flux we obtained for sequence 160062 is consistent with that inferred by Belloni et al. (1993). The source was also detected during sequence 160061 (see Table 1).

For each *ROSAT* observability window of GS 0834−43 we obtained an independent source position. These were determined to be RA = $08^h35^m55\overset{s}{.}6$, Dec. = $-43°11'07\overset{''}{.}3$ (sequence 160061: 1991 May; equinox 2000), and RA = $08^h35^m55\overset{s}{.}2$, Dec. = $-43°11'10\overset{''}{.}3$ (sequence 500127–8: December 17–21; equinox 2000). The statistical uncertainty corresponds to error radii of only 0.5 and 0.2 arcsec for May 5 and December 17–21, respectively (90 per cent confidence level). However, owing to the uncertainty in the boresight correction, the error radius increases to 10 arcsec. We excluded sequence 160062 from our position analysis, as the source was close to the circular support rib (radius of ~20 arcmin) of the PSPC, resulting in a higher uncertainty (error radius of ≳20 arcsec). We note that the new refined positions of GS 0834−43 lie about ~18 arcsec (160061) and ~15 arcsec (500127–8) away from that obtained from sequence 160062 (Belloni et al. 1993; error radius 9 arcsec).

The *ROSAT* event list and spectra of GS 0834−43 were extracted from a circle around the best X-ray position (with an extraction radius corresponding to an encircled energy of 90 per cent at the relevant off-axis angle). The photon arrival times were corrected to the barycentre of the solar system and a background corrected 1-s binned light curve accumulated for each observation. In order to maximize the period search sensitivity we analysed only the observation with the highest statistics, namely sequence 500127–8 merged. A power spectrum was calculated over the entire observation duration following the method described by Israel & Stella (1996). To increase the search sensitivity, we searched for significant peaks in a narrow period interval centred around the period value detected by BATSE between 1991 December 28 and 1992 January 2 (Wilson et al. 1997; 12.307 s), thus only a few days after the *ROSAT* observation. We found a significant peak at a confidence level of 99.5 per cent at a period of 12.307 ± 0.003 s (90 per cent uncertainties are used through out this paper). The pulsed fraction is 7 ± 2 per cent, while the 0.1–2.4 keV pulse shape is well fitted by two sinusoidal waves (see Fig. 1). A similar shape and pulsed fraction value were obtained at

Table 1. *ROSAT* and *ASCA* observations of GS 0834−43.

Pointing number	Instr.	Exposure (s)	Start time	Stop time	Count rate[a] (count s^{-1})	Off-axis angle (arcmin)	Coordinates[b]
500015	PSPC	1854	1991 Apr 25 13:05	1991 Apr 25 13:30	<0.20	44	–
160062	PSPC	2191	1991 May 05 16:41	1991 May 05 17:18	0.510 ± 0.025	22	see Belloni et al. (1993)
160061	PSPC	2005	1991 May 05 19:46	1991 May 05 20:21	0.067 ± 0.018	0	RA = $08^h35^m55\overset{s}{.}6$ Dec. = $-43°11'07\overset{''}{.}3$
500015	PSPC	8666	1991 May 06 06:40	1991 May 06 14:58	<0.11	44	–
500128	PSPC	1316	1991 Dec 04 01:19	1991 Dec 04 01:41	0.237 ± 0.023	12	–
500127–8	PSPC	18235	1991 Dec 17 11:31	1991 Dec 21 08:38	1.137 ± 0.019	12	RA = $08^h35^m55\overset{s}{.}2$ Dec. = $-43°11'10\overset{''}{.}3$
42023000	GIS	35916	1994 Nov 28 07:45	1994 Nov 28 19:01	<0.01	10	–

[a] *ROSAT* PSPC and *ASCA* GIS locally background-corrected count rates were obtained in the 0.5–2.0 keV and 0.5–10 keV energy bands, respectively. The *ROSAT* PSPC count rates are vignetting and PSF-corrected. Errors are at the 1σ level while upper limits are at the 3σ level.
[b] Equinox 2000. Error radius of 10 arcsec at 90 per cent confidence level.

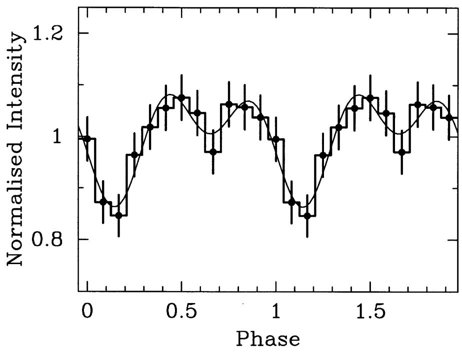

Figure 1. The 1991 December 17–21 *ROSAT* PSPC light curve folded at the best period $P = 12.307$ s.

Table 2. *ROSAT* PSPC spectral results for GS 0834−43.

Parameter	May 1991 (160062)	May 1991 (160061)	Dec 1991 (500127–8)
	Power-law model		
N_H (10^{22} cm^{-2})	$2.3^{+0.5}_{-0.3}$	$1.1^{+0.8}_{-0.4}$	$2.3^{+0.5}_{-0.3}$
Γ	0.7 (fixed)	0.7 (fixed)	0.7 ± 0.7
F_X (10^{-11})	1.73	0.17	5.46
L_X ($N_H = 0$; 10^{35})	2.58	0.13	8.05
	Blackbody model		
N_H (10^{22} cm^{-2})	$2.0^{+0.5}_{-0.3}$	$0.8^{+0.8}_{-0.4}$	$2.0^{+0.3}_{-0.2}$
kT (keV)	1.0 (fixed)	1.0 (fixed)	$1.0^{+0.4}_{-0.3}$
F_X (10^{-11})	1.71	0.16	5.44
L_X ($N_H = 0$; 10^{35})	1.781	0.10	5.50
Radius (km @ 5 kpc)	9.2	2.1	16.7

Note: the X-ray fluxes (units are erg cm^{-2} s^{-1}) and the unabsorbed luminosities (units are erg s^{-1}; a distance of 5 kpc was assumed) refer to the 0.1–2.4 keV energy band.

higher energies in 1991 December by BATSE (see figs 5, 11 and 12 of Wilson et al. 1997).

The PSPC pulse height analyser (PHA) rates were grouped so as to contain a minimum of 20 photons per energy bin. The spectra of sequences 160062, 160061 and 500127–8 (December 17–21) were fitted simultaneously. By using the brightest spectrum parameters as templates, we fitted the three data sets, keeping fixed the photon index and the temperature of the power law and blackbody, respectively, for the two fainter spectra. A power law ($\Gamma = 0.7$) as well as a blackbody ($kT = 1$ keV) model gave good fits ($\chi^2_\nu = 1.09$ and $\chi^2_\nu = 1.11$, respectively).

The field of GS 0834−43 was also observed on 1994 November 28 with the *ASCA* satellite. The source was not detected in the 0.5–10 keV band and a 3σ upper limit of 0.01 count s^{-1} was inferred (corresponding to $\sim 4 \times 10^{-13}$ erg s^{-1} cm^{-2} assuming the best power-law model parameters of Table 2).

3 OPTICAL FOLLOW-UP

Based on the new X-ray positions, we carried out an optical follow-up from the ESO (La Silla, Chile) on 1999 January 18–20 with the 1.5-m Danish telescope and on March 13 with the New Technology Telescope (NTT).

Imaging and photometry in *V*, *R* and Gunn *i* bands (200 s exposure time each) were performed on 1999 January 18–19 with the Danish Faint Object Spectrometer Camera (DFOSC), while spectroscopy of the brightest stars within the X-ray position uncertainty regions was obtained with the same instrument on 1999 January 19–20. The data were reduced using standard ESO–MIDAS procedures for bias subtraction, flat-field correction, aperture photometry and one-dimensional stellar and sky spectra extraction. Profile-fitting photometry was also carried out with DAOPHOT II (Stetson 1987). Cosmic rays were removed from each frame, and the spectrum corrected for the atmospheric extinction and flux-calibrated. Fig. 2 shows the field of GS 0834−43 in the *R* filter (left panel) with the new X-ray uncertainty circles obtained from the 1991 May and December *ROSAT* observations superimposed. The earlier X-ray error circle (labelled as OLD) is also shown. Stars A and C lie outside the new uncertainty regions (~2 and ~6 arcsec away, respectively) while star D is the only object consistent with both circles; it is located at RA = $08^h35^m55\overset{s}{.}4$ and Dec. = $-43°11'11\overset{''}{.}9$ (equinox 2000; calibrated with DSS1 plates; uncertainty 1 arcsec). Photometry measurements for stars A, B, C and D are reported in Table 3.

Since the spectroscopic properties of star A were investigated by Belloni et al. 1993 (star A is a late spectral type star without any significant emission features), we focused our attention on star D. We obtained three low-resolution (11 Å) spectra (30 min exposure time each; 1.5 arcsec slit; 1.2 arcsec seeing) of star D on 1999 January 20 with a grism covering the spectral range 5200–10000 Å (see upper line of Fig. 3). Note that the blue part of the spectrum, being relatively faint ($V = 20.4$), was below the instrument sensitivity (telescope + CCD + grism). After reduction, the spectra were summed to increase the S/N ratio. Star D was also observed on 1999 March 13 with the ESO multimode instrument (EMMI) mounted on the adaptor–rotator at the Nasmyth B focus of the NTT. A 30-min low-resolution (11 Å; 2 arcsec slit; 2 arcsec seeing) spectrum was obtained in the 4000–8500 Å range (see Fig. 3; lower line).

Owing to its faintness, star D is difficult to study. The S/N ratio of the summed DFOSC spectrum is acceptable only above ~6000 Å, while at >7500 Å the signal is dominated by interference fringes. The steep rise of the spectrum in the UV argues for a very hot and reddened object. The absence of strong forbidden lines rules out the possibility of a pre-main sequence object or a cataclysmic variable. Moreover, the absence of strong absorption features points to an OB spectral type star. The main features of the DFOSC spectrum are (i) a strong Hα emission line with equivalent width EW $\sim -30 \pm 2$ Å, and (ii) pronounced interstellar absorption lines for Na II (5890 and 6270 Å). The Hα line shows an extended and asymmetric profile. At 11 Å spectral resolution, this might indicate a line splitting, possibly caused by the presence of a disc. All this evidence clearly points to the association of this object with the X-ray source.

The EMMI spectrum has a slightly better S/N ratio and allows us to extend the spectral region into the 5500–8400 Å range. However, a precise spectral classification is not yet possible. A few Si II lines (e.g. the strong 5466.43–5466.87 Å doublet) are recognizable, suggesting a B2 spectral type. However the uncertainty in the spectral classification is large, ranging from an O8e to a B3e star. Emission features corresponding to He I lines (e.g. 6678 and 7281 Å) are also evident, while the He I lines at 7065 and 7818 Å look filled in, as well as faint nebular [N II] lines on both sides of Hα, which are most likely caused by the superposed emission from the Vela SNR (see Fig. 3). In the EMMI spectrum, the Hα EW is -33 ± 2 Å, while the full width at zero height (FWZH) is 41 ± 3 Å, corresponding to a stellar wind terminal velocity $V_{wind} \simeq 1800$ km s^{-1}. Deep interstellar lines and bands are clearly visible in the star spectra, the Na D2 doublet having an EW of 4.1 ± 0.8 Å.

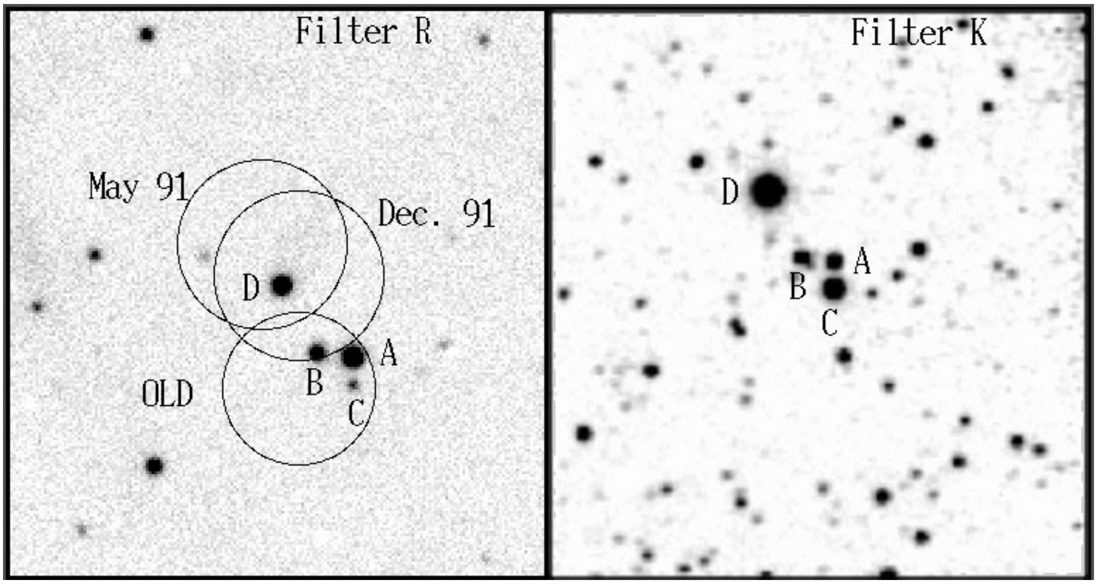

Figure 2. *R*-band (left) and K'-band (right) images of the field of GS 0834 − 43, together with the new X-ray position uncertainty regions (10 arcsec radius) obtained with the 1991 *ROSAT* PSPC observations. North is top, east is left. Star D represents the proposed optical counterpart of GS 0834−43.

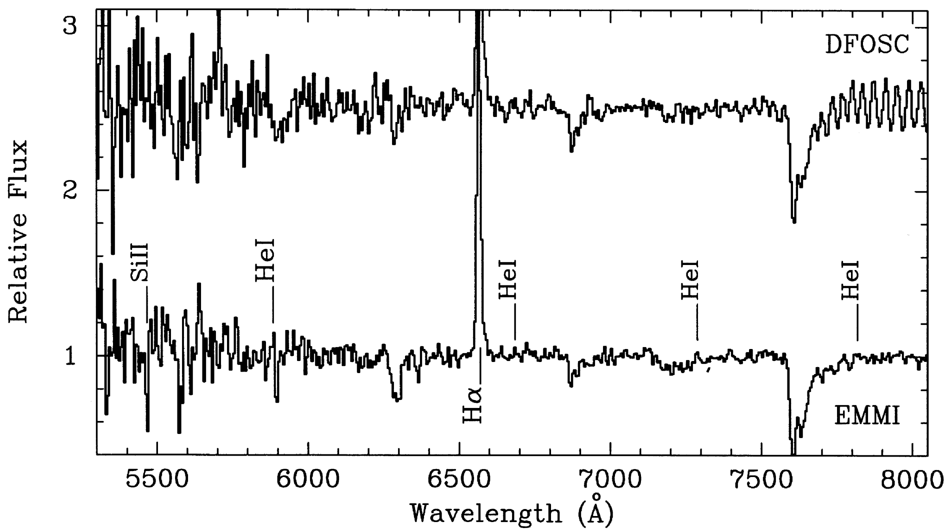

Figure 3. Low-resolution spectra of GS 0834−43 obtained on 1999 January 20 (upper line; Danish + DFOSC) and March 13 (lower line; NTT+EMMI). Fluxes are arbitrarily normalized and a constant was added to the January 20 data.

Table 3. Optical and IR results for stars A, B, C and D.

Star	V	R	$V-R$	J	H	K'	$J-K'$
A	18.9	17.8	1.1	15.86	15.06	14.80	1.06
B	20.4	19.0	1.4	16.20	15.24	14.98	1.22
C	22.9	20.8	2.1	15.40	13.81	13.29	2.11
D	20.4	18.2	2.2	13.33	12.26	11.39	1.94

Note: optical magnitude absolute uncertainty is ~0.2, IR uncertainty is ~0.02.

Star B, the position of which is still marginally consistent with the new X-ray error circle, was observed on 1999 January 19. We obtained a low-resolution (11 Å) spectrum (1 h exposure time; 2.0 arcsec slit; 1.7 arcsec seeing) with a grism covering the 3500–7000 Å spectral range. Star B is even more difficult to study, being fainter than star D. Although the spectrum has a low S/N ratio, we detected large and deep absorption features typical of late-type stars (probably an early M). Moreover, no emission lines were visible in its spectrum.

4 IR OBSERVATIONS

Infrared observations were carried out on 1993 April 1 during service observing time using the Infrared Imager Spectrograph (IRIS) instrument (Allen 1993) mounted at the Cassegrain focus of the 3.9-m Anglo–Australian Telescope (AAT), Siding Springs Observatory, New South Wales. Images were obtained in the *J* (60 s), *H* (20 s) and K' (5 s) bands. The data were reduced using the Starlink FIGARO software (Shortridge et al. 1998), and analysed using the PHOTOM package (Eaton & Draper 1998). The standard stars HD 84090 and HD 100231 were used for calibration purposes, giving absolute uncertainties of around 0.02 mag in each band (although the *H*-band image was near the saturation limit of the detector and should be treated with a little more suspicion).

Taking the colours of a B2V star from Wegner (1994) as $(V-K) = -0.67$, $(J-K) = -0.18$ and $(H-K) = -0.04$, using the reddening relationships, which give $E(J-K)/E(B-V) = +0.50$, and combining these with the observed values for GS 0834−43, we find $E(J-K) = +2.0$ and thus $E(B-V) = +4.0$. Taking the parameter $R_{\rm ext} = 3.3$ [$R_{\rm ext} = A_V/E(B-V)$], we estimate an extinction of $A_V = 13.2$ from the IR magnitudes.

5 DISCUSSION

The X-ray, optical and IR observations of the field of GS 0834−43 presented here led to the identification of the optical counterpart of this 12-s transient X-ray pulsar discovered in 1990. The measurement of the distance to GS 0834−43 based on the optical data is hampered by the uncertainties in the spectral classification.

However, some information can be inferred based on our optical and IR photometric measurements. The intrinsic $V-R$ colour for GS 0834−43 is ~ -0.1 (assuming a main-sequence star with spectral type in the O9–B3 range). As the observed $V-R$ is $\sim$2.25, the reddening should amount to $E_{V-R} \sim 2.35$, and assuming a standard reddening law (Fitzpatrick 1999) this converts to $A_R \sim 7$ (regardless of whether the reddening medium is uniformly distributed along the line of sight or is intrinsic to the source). Moreover, from the X-ray spectral fits, we derive a $N_{\rm H}$ of $1\text{–}2 \times 10^{22}$, which is in good agreement with the photometric reddening estimate (Bohlin, Savage & Drake 1978). The observed magnitude of GS 0834−43 is $R \sim 18.2$ and the absolute R magnitude of a star with the assumed spectral type is between -2.5 and -5. Taking into account the effects of reddening, a distance modulus within the range 13.7–16.2 can be derived. This translates to a distance of ∼5–17 kpc, well beyond the Vela SNR located at ∼500 pc. However, the Galaxy edge in the direction of GS 0834−43 is located at ∼6 kpc, so we can put a limit on the spectral type of star D, assuming that it is placed at the Galactic border. For an O9, B0 or B2 dwarf star we obtain a reddened ($A_R \sim 7$) R magnitude at 6 kpc (distance modulus of ∼14) of 16.5, 17 and 18.5, respectively. When compared with the observed R magnitude of 18.2 for star D, this suggests a B2Ve spectral type star.

Also, the derived $E(B-V) = +4.0$ from the IR data suggests a highly reddened object. Using the relationship for the contribution of the circumstellar (cs) environment derived by Fabregat & Reglero (1990), where $E_{\rm cs} = 0.0049\text{–}0.00185\,{\rm EW(H}\alpha)$, and given the observed ${\rm EW(H}\alpha) \sim -30$ Å, we estimate $E_{\rm cs}$ to be only 0.06 mag. This suggests that the bulk of the extinction is interstellar rather than local to GS 0834−43. This results confirm that the contribution of the disc (which is clearly present, given the large equivalent width inferred for Hα) to the observed IR colours is relatively small.

However, the value of $A_V \sim 13$ derived from the IR observations differs significantly from that estimated from the optical data (where $A_R \sim 7$, and thus $A_V \sim 9.4$), suggesting that the object is either earlier in spectral class than B2, closer than 5–6 kpc, or possibly not a main-sequence object. The observed magnitudes are similar to those of EXO 2030+375 (see e.g. Negueruela 1998), which is compatible with a B0V star at ∼3 kpc or a B0III at ∼5 kpc.

Based on both photometric and spectroscopic findings, we conclude that star D is most likely a B0–2 V–IIIe star at a distance of 3–5 kpc. A more accurate distance and spectral classification will have to await detailed optical spectroscopic observations at the blue end of the spectrum.

For a distance of 5 kpc and extrapolating the 0.1–2 keV *ROSAT* fluxes to the 1–10 keV band (we assume the spectral model fitted by Aoki et al. 1992 using *Ginga* data), we obtain an outburst peak luminosity $L_{\rm X}(1\text{–}10\,{\rm keV}) \simeq 5\text{–}8 \times 10^{36}\,{\rm erg\,s^{-1}}$. A somewhat higher luminosity ($\simeq 10^{37}\,{\rm erg\,s^{-1}}$) would be inferred by extrapolating the 20–100 keV BATSE peak flux reported by Wilson et al. (1997) to the 1–10 keV band. Such a peak luminosity is a typical value shown by X-ray pulsars that also display Type I outbursts (Stella et al. 1986; Negueruela 1998) occurring close to the time of periastron passage and with a periodic recurrence given by the orbital period of the system.

ACKNOWLEDGMENTS

This work was partially supported through an ASI grant. PR thanks the service observing programme of the AAO. This work was partially based on observations carried out at ESO, La Silla, Chile (62.H–0513).

REFERENCES

Allen D., 1993, IRIS Users Manual, Anglo-Australian Observatory manual 30a, version 2.5,
Aoki T. et al., 1992, PASJ, 44, 641
Belloni T., Hasinger G., Pietsch W., Mereghetti S., Bignami G. F., Caraveo P., 1993, A&A, 271, 487
Bohlin R. C., Savage B. D., Drake J. F., 1978, ApJ, 224, 132
Campana S., Lazzati D., Panzera M. R., Tagliaferri G., 1999, ApJ, 524, 423
Eaton N., Draper P. W., 1998, Starlink User Note 45.8, PHOTOM Users guide version 1.7
Fabregat J., Reglero V., 1990, MNRAS, 247, 407
Fitzpatrick E. L., 1999, PASP, 111, 63
Grebenev S., Sunyaev R., 1991, IAU Circ. 5294,
Hasinger G., Pietsch W., Belloni T., 1990, IAU Circ. 5142
Israel G. L., Stella L., 1996, ApJ, 468, 369
Lazzati D., Campana S., Rosati P., Panzera M. R., Tagliaferri G., 1999, ApJ, 524, 414
Makino F., 1990a, IAU Circ. 5142
Makino F., 1990b, IAU Circ. 5139
Makino F., 1990c, IAU Circ. 5148,
Negueruela I., 1998, A&A, 338, 505
Shortridge K. et al., 1998, Starlink User Note 86.16, FIGARO Users guide version 5.4-0
Stella L., White N. E., Rosner R., 1986, ApJ, 208, 669
Stetson P. B., 1987, PASP, 99, 191
Stevens J. B., Coe M. J., Buckley D. A. H., 1999, MNRAS, 309, 421
Sunyaev R., 1990, IAU Circ. 5122
Wegner W., 1994, MNRAS, 270, 229
White N. E., Nagase F., Parmar A. N., 1995, in Lewin W. H. G., van Paradijs J., van den Heuvel E. P. J., eds, X-ray Binaries. Cambridge Univ. Press, Cambridge, p. 1
Wilson C. A., Finger M. H., Harmon B. A., Scott D. M., Wilson R. B., Bildsten L., Chakrabarty D., Prince T. A., 1997, ApJ, 479, 388

This paper has been typeset from a TEX/LATEX file prepared by the author.